

Offshell effects in electromagnetic reactions on the deuteron [†]

Michael Schwamb and Hartmuth Arenhövel

Institut für Kernphysik, Johannes Gutenberg-Universität, D-55099 Mainz, Germany

Offshell contributions to the electromagnetic nuclear current are evaluated within a nonrelativistic approach by incorporation one-pion loop contributions in time-ordered perturbation theory. By construction, the correct experimental onshell properties of the nucleon current are ensured so that only the genuine offshell effects appear as model dependent. For a qualitative assessment of such offshell effects, this model is applied to photodisintegration of the deuteron for photon energies up to 500 MeV. While at low energies offshell contributions are small, above 300 MeV they lead to sizeable effects in observables up to about 30 percent pointing to the necessity of incorporating such effects if one aims at theoretical predictions of high precision.

I. INTRODUCTION

The electromagnetic probe provides one of the most important and accurate tools for the study of nuclear or more general hadron structure. The probing operator hereby is the electromagnetic current of the system, and thus its knowledge is essential for unraveling the internal dynamics. The leading contribution is provided by the one-body currents of the constituents supplemented by additional interaction currents, in general of many-body type.

The one-body nucleon current has the well-known onshell form

$$\langle N\vec{p}' | j^\mu(q) | N\vec{p} \rangle = e \bar{u}(p') \left[F_1(q^2) \gamma^\mu + i \frac{F_2(q^2)}{2M_N} \sigma^{\mu\nu} q_\nu \right] u(p), \quad (1)$$

where e denotes the elementary charge. This form follows from general principles, i.e., Lorentz covariance, time, parity and gauge invariance, provided the nucleon in the initial and final state is on mass shell. The Dirac and Pauli form factors, $F_1(q^2)$ and $F_2(q^2)$, respectively, reflect the internal structure of the nucleon. In other words, nucleon degrees of freedom (d.o.f.) are not the fundamental d.o.f. but effective d.o.f. These form factors are determined by the nucleon's charge and magnetization densities and can be measured experimentally in elastic electron-nucleon scattering, leaving aside the problem associated with the absence of free neutron targets. It is convenient to exhibit explicitly their isospin dependence

$$F_i = \frac{1}{2} (F_i^s + \tau_0 F_i^v). \quad (2)$$

At the photon point the form factors are normalized according to

$$F_1^s(0) \equiv e_{phys}^s = 1, \quad F_1^v(0) \equiv e_{phys}^v = 1, \quad F_1^s(0) \equiv \kappa_{phys}^s = -0.12, \quad F_1^v(0) \equiv \kappa_{phys}^v = 3.70, \quad (3)$$

where e_{phys}^s , e_{phys}^v , κ_{phys}^s , and κ_{phys}^v denote the isoscalar (s) and isovector (v) parts of charge and anomalous magnetic moment, respectively.

The problem of offshell continuation arises if one incorporates this current into reactions which involve an offshell nucleon. For example, in electromagnetic pion production on the nucleon, the nucleon pole diagram contains an intermediate offshell nucleon. Other examples are provided by electromagnetic reactions on nuclei. In this case, a nucleon interacting with the photon is bound inside the nuclear environment and thus is necessarily offshell. Furthermore, the struck nucleon is exposed to final state interaction effects afterwards so that in general the nucleon is offshell both in the initial and final states. Therefore, such reactions call for a generalization of the onshell current of (1) to the offshell case.

About forty years ago, it has been shown by Bincer [1], that the corresponding offshell current contains in general twelve instead of only two form factors which, moreover, do depend not only on the photon

[†]Supported by the Deutsche Forschungsgemeinschaft (SFB 443).

momentum q but also on the invariant masses W and W' of the initial and final nucleon, respectively. Due to the complexity of this offshell current and the fact that one needs a theoretical model for it, one usually neglects in theoretical calculations such offshell effects. The crucial question, however, remains whether this approximation is sufficiently accurate with respect to the accuracy of experimental data to be compared with. In particular, for polarization observables, which play an increasing role in present state-of-the-art nuclear physics, it is well known that even “small” reaction mechanisms like offshell effects may become important.

In the literature, the problem of offshell form factors in the γN -vertex has been faced in different ways. They are based either on dispersion theory [2–4], on chiral perturbation theory [5] or on one-pion loop models [6–9]. Quantitatively, these approaches yield quite different results. For example, as has been stressed in [10], at the photon point the various predictions for the slope of the offshell continuation F^{++} of the onshell Pauli form factor taken at the onshell point

$$\left. \frac{\partial F^{++}(q^2 = 0, W, W')}{\partial(W/M_N)} \right|_{W=W'=M_N} \quad (4)$$

differ in magnitude and even in sign. Thus at present, these numbers should only be considered as an illustration. But a more quantitative estimate of offshell effects in electromagnetic reactions is still missing. Moreover, one should keep in mind that offshell effects are not only model but also representation dependent and as such are not observable directly. This has been stressed recently by Fearing and Scherer [11,12], who have proven the impossibility of *measuring* off-shell effects unambiguously in nucleon-nucleon bremsstrahlung and related processes.

With respect to the study of offshell effects in electromagnetic reactions on nuclei, we would like to mention first the work of Naus and Koch [6], who have calculated the e - N cross section for a bound nucleon making some simplifying assumptions about the wave function and the current structure. Within their framework, which did not contain any nuclear dynamics, they obtained by offshell effects an increase of about 8 % in the cross section. Similarly, Tiemeijer and Tjon [7] estimated offshell effects to be of the order of a few percent only in elastic and inelastic photon scattering off a nucleus. On the other hand, Song et al. [13] obtained a reduction of the longitudinal response function R_L for ^{12}C up to about 20 % by electromagnetic offshell effects using a relativistic Fermi-gas model. Last but not least, we would like to mention the recent work of Kondratyuk and collaborators [10,14]. In [10], offshell effects were investigated in proton-proton bremsstrahlung using a parameterization of the offshell form factors based on their general properties and consistent with the above mentioned model calculations [8,9]. Quite important offshell effects were found, especially for the analyzing power, which where of the order of about 25 - 30 %. On the other hand, in [14] a microscopic model for the half offshell γN -current has been presented by dressing the γN -vertex with pion loops. By implementing the latter in a K -matrix approach to the Compton scattering amplitude on the nucleon, the authors found a sizeable enhancement of up to about 10 % for the forward cross section above the π -threshold.

In view of the fact, that all the approaches to offshell effects in electromagnetic reactions on nuclei lack a certain degree of consistency, since the underlying dynamical origin of such offshell effects is certainly related to the mechanisms responsible for the NN -interaction, we would like to present in this paper a study of offshell effects in electromagnetic reactions on the deuteron, where we try to be as consistent as possible with respect to the dynamical input. Therefore, we use a three-body approach, described in detail in [15,16], whose basic interactions, apart from other contributions not important for the forthcoming discussion, consist of meson-nucleon vertices, electromagnetic baryonic and mesonic one-body currents as well as the vertex- and the Kroll-Rudermann contribution. These interactions are the basic building blocks of the corresponding effective operators like the retarded NN -interaction and retarded MEC as well as the hadronic and electromagnetic loop corrections. The incorporation of the latter lead directly to the desired offshell contributions to the electromagnetic one-body current as will be outlined in the next sections. Due to our framework, they contain for example the same πN -vertex like the π -MEC or the one-pion-exchange NN -potential.

The choice of the deuteron is motivated by the fact that the deuteron is the simplest nucleus serving as an ideal laboratory for the study of the relevant mechanisms of the strong interaction. A variety of such mechanisms like meson exchange currents and isobar configurations have first been studied for the deuteron. For these reasons, we can expect that offshell effects in the γN -vertex can be studied most reliably for reactions on this nucleus. Moreover, the question of offshell effects in the deuteron is also relevant with respect to its use as a neutron target in order to determine neutron properties like, e.g., its

electric form factor. Since however, the neutron bound in the deuteron is not onshell, one has to assess, among other things, the size of possible offshell modifications. Another topic of current interest in this respect is the proposed measurement (at MAMI in Mainz and ELSA in Bonn) of the spin asymmetry and the GDH-sum rule of the deuteron in order to test our knowledge of the spin asymmetry of the neutron.

In order to simplify the discussion, we will consider in this work only real photons. Moreover, we have selected for this study as basic process the simplest photonuclear reaction on a nucleus, i.e. deuteron photodisintegration. The study of more complicated processes like electrodisintegration or pionproduction is devoted to forthcoming papers.

As has been mentioned above, we take as theoretical framework a previously developed nonrelativistic time ordered perturbation approach based on a model with explicit meson, nucleon, and isobar d.o.f. [15,16]. Similar to [6,7], we calculate the offshell effects in the nucleon one-body current by evaluating a one-pion loop contribution. We are aware of the fact that the size of offshell effects will be model dependent. However, at present we consider the adopted treatment realistic enough in order to find at least a semiquantitative answer to the question, whether offshell effects in electromagnetic reactions on the deuteron are in general negligible or have to be included. If the latter turns out to be true, one certainly has to refine the present model in the future towards a more quantitative treatment of such effects. Comparing the general structure of our model with the approach in [6,7], we would like to point out at least two major differences. Whereas in [6,7] a fully relativistic framework has been adopted, we use a nonrelativistic model. It allows us to study offshell effects *consistently* within a realistic interaction model which is suitable for energies not only below, but also above π -threshold, where the Δ isobar plays an important role. Moreover, due to a specific renormalization scheme, which will be described in detail below, we guarantee that the experimental onshell properties of the nucleon current are preserved in our model. Only the offshell continuation of the current is model dependent. As we will see in detail, this treatment allows us to preserve the good description of deuteron photodisintegration of [16]. Such a scheme has not been applied in [6,7], where the offshell as well as the onshell form factors have been calculated within the same framework. Due to the simplicity of the one-pion loop model, the onshell values did not reproduce the experimental ones. For example, Naus and Koch [6] obtained $\kappa_{phys}^s = -3.19$ and $\kappa_{phys}^v = 4.21$, whereas the vector dominance model adopted by Tiemeijer and Tjon [7] yielded $\kappa_{phys}^s = -0.34$ and $\kappa_{phys}^v = 3.82$ for pseudovector πN -coupling which are closer to experiment.

In Sects. II and III, we briefly describe the general framework of [15,16] which we use in the present study. It allows to incorporate completely retardation effects in potentials and meson exchange currents, and we consider it suitable for the description of photoreactions in the energy range up to about $k_{lab} = 500$ MeV. The model for evaluating offshell effects in the electromagnetic one-body current is described in Sect. IV. In Sects. V and VI, we discuss the predictions for a variety of observables and compare them to experimental data where available. In the last section VII, we will draw some conclusions and give an outlook for future studies.

II. REVIEW OF THE THEORETICAL FRAMEWORK

The model Hilbert space consists of three orthogonal subspaces

$$\mathcal{H}^{[2]} = \mathcal{H}_N^{[2]} \oplus \mathcal{H}_\Delta^{[2]} \oplus \mathcal{H}_X^{[2]}, \quad (5)$$

where $\mathcal{H}_N^{[2]}$ contains two bare nucleons, $\mathcal{H}_\Delta^{[2]}$ one nucleon and one $\Delta(1232)$ -resonance, and $\mathcal{H}_X^{[2]}$ two nucleons and one meson $X \in \{\pi, \rho, \sigma, \delta, \omega, \eta\}$. Thus the latter can be divided further into subspaces corresponding to the different mesons

$$\mathcal{H}_X^{[2]} = \sum_{i \in \{\pi, \rho, \sigma, \delta, \omega, \eta\}} \mathcal{H}_{X_i}^{[2]}. \quad (6)$$

In order to distinguish the various sectors of $\mathcal{H}^{[2]}$, we introduce appropriate projection operators by

$$P_N \mathcal{H}^{[2]} = \mathcal{H}_N^{[2]}, \quad P_\Delta \mathcal{H}^{[2]} = \mathcal{H}_\Delta^{[2]}, \quad P_{X_i} \mathcal{H}^{[2]} = \mathcal{H}_{X_i}^{[2]}. \quad (7)$$

For convenience, we furthermore introduce

$$P = P_{\bar{N}} + P_{\Delta} \quad \text{and} \quad P_X = \sum_{i \in \{\pi, \rho, \sigma, \delta, \omega, \eta\}} P_{X_i}. \quad (8)$$

Using the notation

$$\Omega_{\alpha\beta} = P_{\alpha} \Omega P_{\beta}, \quad \alpha, \beta \in \{\bar{N}, \Delta, X\}, \quad (9)$$

any operator Ω acting in $\mathcal{H}^{[2]}$ can be written as a symbolic 3×3 matrix

$$\Omega = \begin{pmatrix} \Omega_{\bar{N}\bar{N}} & \Omega_{\bar{N}\Delta} & \Omega_{\bar{N}X} \\ \Omega_{\Delta\bar{N}} & \Omega_{\Delta\Delta} & \Omega_{\Delta X} \\ \Omega_{X\bar{N}} & \Omega_{X\Delta} & \Omega_{XX} \end{pmatrix}. \quad (10)$$

The hamiltonian H is subdivided into a kinetic part H_0 , containing the physical mass of the nucleon, and into an interaction part V^0 . As outlined in detail in [15], V^0 comprises besides baryon-meson vertices a two-body interaction $V_{PP}^{0[2]}$, characterized by a superscript “[2]” and represented diagrammatically in Fig. 1, and furthermore a counter term $V^{[c]}$ taking into account the nonvanishing mass difference between a bare and a physical nucleon. Any hadronic state $|\bar{\alpha}\rangle$ can be written as a sum of a “baryonic” part $P|\bar{\alpha}\rangle$ and a “mesonic” part $P_X|\bar{\alpha}\rangle$. For an eigenstate $|\bar{\alpha}_E\rangle$ of the Hamilton operator

$$H|\bar{\alpha}_E\rangle = E|\bar{\alpha}_E\rangle, \quad (11)$$

the two components are related by

$$P_X|\bar{\alpha}_E\rangle = G^X(E + i\epsilon)V_{XP}^0|\bar{\alpha}_E\rangle, \quad (12)$$

where $G^X(z)$ describes the propagation of two interacting nucleons in the presence of a spectator meson

$$G^X(z) = (z - H_{0,XX} - V_{XX}^0)^{-1}. \quad (13)$$

The baryonic component $P|\bar{\alpha}_E\rangle$ is obtained as solution of a Schrödinger like equation

$$(H_0 + V_{PP}^0 + V_{PX}^0 G^X(z) V_{XP}^0) P|\bar{\alpha}_E\rangle = E P|\bar{\alpha}_E\rangle. \quad (14)$$

Note that V_{PP}^0 as well as $V_{PX}^0 G^X(z) V_{XP}^0$ consist of a connected (*con*) and a disconnected (*dis*) part,

$$V_{PP}^0 = V_{PP}^{0,dis} + V_{PP}^{0,con}, \quad V_{PP}^{0,dis} \equiv V_{PP}^{[c]}, \quad V_{PP}^{0,con} \equiv V_{PP}^{0[2]}, \quad (15)$$

$$V_{PX}^0 G^X(z) V_{XP}^0 = [V_{PX}^0 G^X(z) V_{XP}^0]_{dis} + [V_{PX}^0 G^X(z) V_{XP}^0]_{con}. \quad (16)$$

As has been discussed in [15], the disconnected pieces contain by definition in general only those parts of the potential which do not describe an interaction between the two baryons. The only exception is the πN loop contribution to the Δ self energy, which we have incorporated into the connected part, containing otherwise the genuine baryon-baryon interactions.

Now, renormalized baryon-baryon and meson-baryon interactions are introduced by (consider for example [17,18])

$$V_{PP}^{[2]} = (\widehat{Z}_{[2]}^{os})^{-1} V_{PP}^{0[2]} (\widehat{Z}_{[2]}^{os})^{-1}, \quad (17)$$

$$V_{XP} = (\widehat{Z}_{[2]}^{os})^{-1} V_{XP}^0 (\widehat{Z}_{[2]}^{os})^{-1}, \quad (18)$$

in order to arrive at an effective description in terms of the renormalized baryonic component

$$|\alpha_E\rangle = \widehat{Z}_{[2]}(E + i\epsilon) P|\bar{\alpha}_E\rangle. \quad (19)$$

Here, the renormalization operator $\widehat{Z}_{[2]}$ and its onshell value $\widehat{Z}_{[2]}^{os}$ are defined by

$$\widehat{Z}_{[2]}^2(z) = 1 + \int dz' \delta(z' - H_0) [V_{\bar{N}X}^0 G_0(z') G_0(z) V_{X\bar{N}}^0]_{dis}, \quad (20)$$

$$(\widehat{Z}_{[2]}^{os})^2 = \int dz \delta(z - H_0) \widehat{Z}_{[2]}^2(z), \quad (21)$$

with

$$G_0(z) = (z - H_0)^{-1}. \quad (22)$$

We have shown in [15], that $\widehat{Z}_{[2]}^{os}$ can be treated within a very good approximation as an energy- and momentum independent constant in $\mathcal{H}_N^{[2]}$. The renormalized interactions (17) and (18) contain renormalized coupling constants which are the relevant physical quantities determined either by experiment or fit to the experimental data. Furthermore, we introduce an auxiliary quantity, namely a “dressing operator”

$$\widehat{R}(z) = \widehat{Z}_{[2]}^{os} \widehat{Z}_{[2]}^{-1}(z), \quad (23)$$

which is equal to the identity for onshell particles. It is diagonal with respect to two-body plane waves

$$\langle \bar{N}(\vec{p}'_1) \bar{N}(\vec{p}'_2) | \widehat{R}(z) | \bar{N}(\vec{p}_1) \bar{N}(\vec{p}_2) \rangle = \delta(\vec{p}'_1 - \vec{p}_1) \delta(\vec{p}'_2 - \vec{p}_2) R(z, \vec{p}_1, \vec{p}_2), \quad (24)$$

with

$$R(z, \vec{p}_1, \vec{p}_2) = \left[1 - \left(z - e_N(p_1) - e_N(p_2) \right) \left(\Gamma_{\vec{p}_1}(z - e_N(p_2)) + \Gamma_{\vec{p}_2}(z - e_N(p_1)) \right) \right]^{-\frac{1}{2}}, \quad (25)$$

where $e_N(p) = \sqrt{M_N^2 + p^2}$ denotes the nucleon onshell energy and $\Gamma_{\vec{p}}$ is defined by

$$\delta(\vec{p}' - \vec{p}) \Gamma_{\vec{p}}(z) = \langle \bar{N}(\vec{p}') | v_{PX\pi}(e_N(p) - h_0)^{-2} (z - h_0)^{-1} v_{X\pi P} | \bar{N}(\vec{p}) \rangle. \quad (26)$$

Here we have exploited the fact that the πN interaction $V_{PX\pi}$ and the free Hamiltonian H_0 can be split into corresponding one-body parts $v_{PX\pi}$ and h_0 , acting in the one-nucleon sector [15].

As has been discussed in detail in [15], one finally obtains from (14) an equation for $|\alpha_E\rangle$

$$H_{eff} |\alpha_E\rangle = E |\alpha_E\rangle \quad (27)$$

where

$$H_{eff} := H_0 + \widehat{R}(E + i\epsilon) \left(V_{PP}^{[2]} + [V_{PX} G^X(E + i\epsilon) V_{XP}]_{con} \right) \widehat{R}(E + i\epsilon) \quad (28)$$

contains renormalized quantities only. For scattering states, $|\alpha_E\rangle$ obeys a corresponding Lippmann-Schwinger equation [15]. In our explicit calculations, we only solve equations like (27) which incorporate physical couplings.

III. THE ELECTROMAGNETIC CURRENT

In this section, we briefly review the general structure of the electromagnetic current, which has been discussed in detail in [16]. We distinguish between three types of currents which are graphically depicted in Figs. 2 through 4. The first type comprises the one- and two-body pure baryon currents, labeled by superscripts “[1]” and “[2]”, respectively. As outlined in [16], the two-body parts describe among other things effective heavy meson exchange currents, which are not generated explicitly via the elementary meson-baryon vertices and the meson production/annihilation currents. The second current type, represented in Fig. 3, comprises the “one-meson production/annihilation” currents consisting of the Kroll-Rudermann contact term $j_{X\bar{N}}^{(0)\mu}$ and a vertex current $j_{X\bar{N}}^{(1)\mu}$, where the lower case letter j from here on always denotes a one-body-current. The third current type is shown in Fig. 4 and describes the coupling of a photon to a meson or nucleon in the presence of two spectator nucleons or one nucleon and one meson, respectively, and the annihilation/creation of two mesons by a photon. One should note that the inclusion of currents depicted in Figs. 3 and 4 allows us to incorporate full π -retardation in the two-body meson-exchange currents.

In view of the effective description in terms of baryonic d.o.f. only, it is useful to introduce an “effective” current operator, acting in pure baryonic space, by

$$\langle \alpha_{E'} | J_{eff}^\mu(z, \vec{k}) | \alpha_E \rangle := \langle \bar{\alpha}_{E'} | J^\mu(\vec{k}) | \bar{\alpha}_E \rangle, \quad (29)$$

where \vec{k} denotes the photon momentum in the c.m. frame. Compared to [16], we have changed our definition of the effective current operator for reasons of convenience. Denoting by $\tilde{J}_{eff}^\mu(z, \vec{k})$ the effective current of [16], one has the relation

$$J_{eff}^\mu(z, \vec{k}) = \frac{\hat{R}(z)}{\hat{Z}_{[2]}^{os}} \tilde{J}_{eff}^\mu(z, \vec{k}) \frac{\hat{R}(z-k)}{\hat{Z}_{[2]}^{os}} \quad (30)$$

to $J_{eff}^\mu(z, \vec{k})$ of (29). Obviously, this change of notation is irrelevant for our numerical results.

The effective current operator can be split into a nucleonic and a resonant part with superscripts “ N ” and “ Δ ”, respectively, which in turn are divided into one- and two-body pieces,

$$J_{eff}^\mu(z, \vec{k}) = J_{eff}^{N[1]\mu}(z, \vec{k}) + J_{eff}^{\Delta[1]\mu}(z, \vec{k}) + J_{eff}^{N[2]\mu}(z, \vec{k}) + J_{eff}^{\Delta[2]\mu}(z, \vec{k}). \quad (31)$$

Their diagrammatic representation is shown in Fig. 5. Except for the effective one-body current $J_{eff}^{N[1]\mu}(z, \vec{k})$, we adopt for all other currents the explicit expressions given in [16] (apart from the above-mentioned change (30) in notation), which therefore are not repeated here. In this context, one should note that offshell contributions have already been implemented in the one-body $\gamma\bar{N}\Delta$ -current $J_{eff}^{\Delta[1]\mu}(z, \vec{k})$ as has been outlined in [16].

The evaluation of the effective nucleonic one-body contribution $J_{eff}^{N[1]\mu}(z, \vec{k})$ is the basic aim of this paper. It will be outlined in the next section.

IV. OFFSHELL CONTRIBUTIONS TO THE NUCLEON ONE-BODY CURRENT

By a straightforward calculation, one obtains for the matrix element of the effective nucleonic one-body current operator $J_{eff}^{N[1]\mu}(z, \vec{k})$ between two eigenstates $|\alpha_W\rangle$ and $|\alpha_{W-k}\rangle$ of H_{eff} (27) with invariant energies W and $W-k$, respectively, the following expression with $z = W + i\epsilon$

$$\langle \alpha_W | J_{eff}^{N[1]\mu}(z, \vec{k}) | \alpha_{W-k} \rangle = \sum_{i=1}^9 \langle \alpha_W | \frac{\hat{R}(z)}{\hat{Z}_{[2]}^{os}} J_i^{N[1]\mu}(z, \vec{k}) \frac{\hat{R}(z-k)}{\hat{Z}_{[2]}^{os}} | \alpha_{W-k} \rangle, \quad (32)$$

where the various terms, represented diagrammatically in Fig. 6, are given by

$$J_1^{N[1]\mu}(z, \vec{k}) = \sum_{i=1,2} j_{\bar{N}\bar{N}}^{[1]\mu}(\vec{k}, i), \quad (33)$$

$$J_2^{N[1]\mu}(z, \vec{k}) = \sum_{i=1,2} v_{\bar{N}X_\pi}^0(i) G_0(z) j_{X_\pi X_\pi}^{\bar{N}\mu}(\vec{k}, i) G_0(z-k) v_{X_\pi \bar{N}}^0(i), \quad (34)$$

$$J_3^{N[1]\mu}(z, \vec{k}) = \sum_{i=1,2} v_{\bar{N}X_\pi}^0(i) G_0(z) j_{X_\pi X_\pi}^{\pi\mu}(\vec{k}) G_0(z-k) v_{X_\pi \bar{N}}^0(i), \quad (35)$$

$$J_4^{N[1]\mu}(z, \vec{k}) = \sum_{i=1,2} j_{\bar{N}X_\pi\pi}^{(0)\mu}(\vec{k}) G_0(z-k) v_{X_\pi\pi X_\pi}^0(i) G_0(z-k) v_{X_\pi \bar{N}}^0(i), \quad (36)$$

$$J_5^{N[1]\mu}(z, \vec{k}) = \sum_{i=1,2} v_{\bar{N}X_\pi}^0(i) G_0(z) v_{X_\pi X_\pi\pi}(i) G_0(z) j_{X_\pi\pi \bar{N}}^{(0)\mu}(\vec{k}), \quad (37)$$

$$J_6^{N[1]\mu}(z, \vec{k}) = \sum_{i=1,2} j_{\bar{N}X_\pi}^{(1)\mu}(\vec{k}, i) G_0(z-k) v_{X_\pi \bar{N}}^0(i), \quad (38)$$

$$J_7^{N[1]\mu}(z, \vec{k}) = \sum_{i=1,2} v_{\bar{N}X_\pi}^0(i) G_0(z) j_{X_\pi \bar{N}}^{(1)\mu}(\vec{k}, i), \quad (39)$$

$$J_8^{N[1]\mu}(z, \vec{k}) = \sum_{i=1,2} j_{\bar{N}X_\pi}^{(1v)\mu}(\vec{k}, i) G_0(z-k) v_{X_\pi \bar{N}}^0(i), \quad (40)$$

$$J_9^{N[1]\mu}(z, \vec{k}) = \sum_{i=1,2} v_{\bar{N}X_\pi}^0(i) G_0(z) j_{X_\pi \bar{N}}^{(1v)\mu}(\vec{k}, i). \quad (41)$$

With respect to these relations, a few remarks are in order. Whereas $J_1^{N[1]\mu}(z, \vec{k})$ is identical to the bare $\gamma\bar{N}$ -current, supplemented by a suitable “counter”-current which will be defined below, the remaining terms describe meson cloud contributions (see Fig. 6). In this work, we restrict ourselves solely to the pion as explicit d.o.f. expecting that heavier mesons, due to their much larger mass, will not change our results and conclusions significantly in the energy region considered here. The contributions $J_4^{N[1]\mu}(z, \vec{k})$ and $J_5^{N[1]\mu}(z, \vec{k})$ contain intermediate two-pion states, which therefore are violating formally our Hilbert space. However, similar to the retarded meson exchange currents discussed in [16], these contributions have to be taken into account in order to guarantee – at least approximately – gauge invariance as is discussed below. All ingredients (vertices, currents) of the meson cloud contributions (35) through (41) are fixed by the corresponding expressions given in [15,16]. Note that the pion-nucleon vertex $v_{X\pi\bar{N}}^0$ contains a dipole form factor with a cutoff mass of 1700 MeV so that the loop integrals do not diverge.

The occurrence of the onshell renormalization operator $\hat{Z}_{[2]}^{os}$ in the matrix element (32) suggests to introduce “renormalized” currents by defining (note the similarity to (17) and (18))

$$J_{i,ren}^{N[1]\mu}(z, \vec{k}) = (\hat{Z}_{[2]}^{os})^{-1} J_i^{N[1]\mu}(z, \vec{k}) (\hat{Z}_{[2]}^{os})^{-1} \quad i \in \{1, \dots, 9\}, \quad (42)$$

so that the corresponding renormalized meson cloud contributions ($i = 2$ through 9 in Fig. 6) contain solely the physical and not the bare pion-nucleon coupling constant. The explicit evaluation of the loops can be performed by using standard techniques (see Appendix A for further details). For the sake of simplicity, we use the nonrelativistic expressions for the pion-nucleon vertex $v_{X\pi\bar{N}}^{0,nonrel}$ and for the momentum-energy relation of the intermediate nucleon which absorbs/emits a pion.

Introducing as a shorthand

$$\mathcal{J}_{loop}^\mu(z, \vec{k}) = \sum_{i=2}^9 J_{i,ren}^{N[1]\mu}(z, \vec{k}) \quad (43)$$

for the renormalized loop contributions, one obtains in general for the matrix element of the latter between two-body momentum eigenstates

$$\begin{aligned} \langle \bar{N}(\vec{p}'_1) \bar{N}(\vec{p}'_2) | \rho_{loop}(z, \vec{k}) | \bar{N}(\vec{p}_1) \bar{N}(\vec{p}_2) \rangle &= e \delta(\vec{p}'_1 - \vec{p}_1 - \vec{k}) \delta(\vec{p}'_2 - \vec{p}_2) \\ &\times \sum_{a=0,1} \sum_{b,c} F^{a,b,c}(z_{sub}(1), p'_1, k) \left[\sigma^{[a]}(1) \times \left[Y^{[b]}(\hat{p}'_1) \times Y^{[c]}(\hat{k}) \right]^{[a]} \right]^{[0]} + (1 \leftrightarrow 2), \\ \langle \bar{N}(\vec{p}'_1) \bar{N}(\vec{p}'_2) | \mathcal{J}_{loop}(z, \vec{k}) | \bar{N}(\vec{p}_1) \bar{N}(\vec{p}_2) \rangle &= e \delta(\vec{p}'_1 - \vec{p}_1 - \vec{k}) \delta(\vec{p}'_2 - \vec{p}_2) \\ &\times \sum_{a=0,1} \sum_{b,c,d} G^{a,b,c,d}(z_{sub}(1), p'_1, k) \left[\sigma^{[a]}(1) \times \left[Y^{[b]}(\hat{p}'_1) \times Y^{[c]}(\hat{k}) \right]^{[d]} \right]^{[1]} + (1 \leftrightarrow 2), \end{aligned} \quad (44)$$

where we use the convention $\sigma^{[0]} \equiv 1$, $k = |\vec{k}|$ and $p' = |\vec{p}'|$. The quantity $z_{sub}(1)$ denotes the offshell-energy of the active nucleon “1” on which the photon is absorbed. In time ordered perturbation theory, $z_{sub}(1)$ is given by $z_{sub}(1) = z - \sqrt{M_N^2 + \vec{p}_2^2}$, where \vec{p}_2 is the momentum of the spectator nucleon “2”. The tensor ranks b, c , and d in (44) are not fixed unambiguously by the underlying fundamental symmetries of the current. In our explicit evaluations, we restrict ourselves to the lowest possible ranks, i.e.

$$\langle \bar{N}(\vec{p}'_1) \bar{N}(\vec{p}'_2) | \rho_{loop}(z, \vec{k}) | \bar{N}(\vec{p}_1) \bar{N}(\vec{p}_2) \rangle = e \delta(\vec{p}'_1 - \vec{p}_1 - \vec{k}) \delta(\vec{p}'_2 - \vec{p}_2) \hat{\alpha}(z_{sub}(1), p'_1, k) + (1 \leftrightarrow 2), \quad (45)$$

$$\begin{aligned} \langle \bar{N}(\vec{p}'_1) \bar{N}(\vec{p}'_2) | \mathcal{J}_{loop}(z, \vec{k}) | \bar{N}(\vec{p}_1) \bar{N}(\vec{p}_2) \rangle &= e \delta(\vec{p}'_1 - \vec{p}_1 - \vec{k}) \delta(\vec{p}'_2 - \vec{p}_2) \left(e \hat{\beta}(z_{sub}(1), p'_1, k) 2\vec{p}'_1 \right. \\ &\left. + e \hat{\gamma}(z_{sub}(1), p'_1, k) \vec{k} + e \hat{\delta}(z_{sub}(1), p'_1, k) i\vec{\sigma} \times \vec{p}'_1 + e \hat{\epsilon}(z_{sub}(1), p'_1, k) i\vec{\sigma}_1 \times \vec{k} \right) + (1 \leftrightarrow 2). \end{aligned} \quad (46)$$

The isospin structure of the scalar functions $\hat{\alpha}, \dots, \hat{\epsilon}$ is parametrized as in (2), e.g.

$$\hat{\alpha} = \frac{1}{2}(\alpha^s + \tau_0 \alpha^v). \quad (47)$$

Due to the occurrence of singularities in the loop diagrams, $\hat{\alpha}, \dots, \hat{\epsilon}$ become complex functions above π -threshold. Therefore, we do not perform a Taylor expansion of these functions with respect to the

arguments k and p'_1 . The term proportional to $\hat{\alpha}$ can be interpreted as an electromagnetic loop correction to the charge of the nucleon. The contributions proportional to $\hat{\beta}$ and $\hat{\gamma}$ correspond to the well-known convection-, the term proportional to $\hat{\epsilon}$ to the spin-current.

Now we will fix the remaining contribution $J_1^{N[1]\mu}(z, \vec{k})$. As already mentioned above, $J_1^{N[1]\mu}(z, \vec{k})$ consists of two parts

$$J_1^{N[1]\mu}(z, \vec{k}) = \sum_{i=1,2} j_{bare}^\mu(i, \vec{k}) + J_{counter}^\mu(\vec{k}), \quad (48)$$

where j_{bare}^μ describes the one-body current of a bare nucleon with the physical charge $\hat{\epsilon}$ and a vanishing anomalous magnetic moment. It is given by

$$\langle \bar{N}(\vec{p}') | \rho_{bare} | \bar{N}(\vec{p}) \rangle = \delta(\vec{p}' - \vec{p} - \vec{k}) \hat{\epsilon}, \quad (49)$$

$$\langle \bar{N}(\vec{p}') | \vec{j}_{bare} | \bar{N}(\vec{p}) \rangle = \delta(\vec{p}' - \vec{p} - \vec{k}) \left\{ \frac{\hat{\epsilon}}{2M_N} (\vec{p}' + \vec{p}) + \frac{\hat{\epsilon} + \hat{\kappa}_{bare}}{2M_N} i \vec{\sigma} \times \vec{k} \right\}, \quad (50)$$

where $\hat{\kappa}_{bare} \equiv 0$. As usual, the isospin structure of the charge operator $\hat{\epsilon}$ is parametrized as

$$\hat{\epsilon} = \frac{e}{2} (1 + \tau_0). \quad (51)$$

Concerning the additional contribution $J_{counter}^\mu$, the simplest treatment obviously would be to set $J_{counter}^\mu \equiv 0$. By this choice, the meson cloud contribution (46) would change the charge of the nucleon and would generate an anomalous magnetic moment which is known to be unrealistic. Moreover, one can show that with this choice gauge invariance is not fulfilled even approximately in the leading order $1/M_N$ (see the discussion below). Therefore, we fix the counter current by requiring that the *onshell* matrix element of the effective one-body nucleonic current $J_{eff}^{N[1]\mu}(z, \vec{k})$ between plane waves is identical to the realistic one-body current $\vec{j}_{real}^{N[1]\mu}$ with the same formal expression as in (49) and (50) except for a nonvanishing anomalous magnetic moment contribution $\hat{\kappa}_{phys}$ of the physical nucleon, i.e.

$$\hat{\kappa}_{bare} \rightarrow \hat{\kappa}_{phys} = \frac{e}{2} (\kappa_{phys}^s + \tau_0 \kappa_{phys}^v) \quad (52)$$

in (50). In detail, this means that the counter current $J_{counter}^\mu$ is defined by requiring

$$\langle \bar{N}(\vec{p}'_1) \bar{N}(\vec{p}'_2) | J_{eff}^{N[1]\mu}(z^{os}, \vec{k}) | \bar{N}(\vec{p}_1) \bar{N}(\vec{p}_2) \rangle = \langle \bar{N}(\vec{p}'_1) \bar{N}(\vec{p}'_2) | \sum_{i=1,2} j_{real}^{N[1]\mu}(i, \vec{k}) | \bar{N}(\vec{p}_1) \bar{N}(\vec{p}_2) \rangle \quad (53)$$

with $z^{os} := e_N(p'_1) + e_N(p'_2)$. We would like to emphasize that this condition allows us to reproduce the physical onshell one-body current no matter what model is used in estimating the loop contributions. In other words, specific approximations of the adopted model like, for example, the neglect of heavier mesons or of two-loop contributions, do not affect the onshell properties of the effective current. Only the offshell continuation of the effective current is model dependent.

A straightforward evaluation of (53) yields for the counter current the expression

$$\begin{aligned} & \langle \bar{N}(\vec{p}'_1) \bar{N}(\vec{p}'_2) | J_{counter}^\mu(\vec{k}) | \bar{N}(\vec{p}_1) \bar{N}(\vec{p}_2) \rangle \\ &= \langle \bar{N}(\vec{p}'_1) \bar{N}(\vec{p}'_2) | - \sum_{i=1,2} j_{bare}^\mu(i, \vec{k}) - \mathcal{J}_{loop}^\mu(z^{os}, \vec{k}) + \frac{\hat{Z}_{[2]}^{os}}{\hat{R}(z^{os})} \sum_{i=1,2} j_{real}^{N[1]\mu}(i, \vec{k}) \frac{\hat{Z}_{[2]}^{os}}{\hat{R}(z^{os} - k)} | \bar{N}(\vec{p}_1) \bar{N}(\vec{p}_2) \rangle \end{aligned} \quad (54)$$

Collecting all pieces, the matrix element of the effective nucleon one-body operator between two-body plane-waves can then be written in the form

$$\begin{aligned} & \langle \bar{N}(\vec{p}'_1) \bar{N}(\vec{p}'_2) | J_{eff}^{N[1]\mu}(z, \vec{k}) | \bar{N}(\vec{p}_1) \bar{N}(\vec{p}_2) \rangle \\ &= \langle \bar{N}(\vec{p}'_1) \bar{N}(\vec{p}'_2) | \frac{\hat{R}(z)}{\hat{R}(z^{os})} \sum_{i=1,2} j_{real}^{N[1]\mu}(i, \vec{k}) \frac{\hat{R}(z - k)}{\hat{R}(z^{os} - k)} + \hat{R}(z) \mathcal{J}_{loop, sub}^\mu(z, \vec{k}) \hat{R}(z - k) | \bar{N}(\vec{p}_1) \bar{N}(\vec{p}_2) \rangle. \end{aligned} \quad (55)$$

Note that, according to (24) through (26), the plane-wave matrix element of $\widehat{R}(z^{os})$ is identical to one (apart from the momentum conserving Delta-function). The matrix element of the current $\mathcal{J}_{loop, sub}^{N\mu}(z, \vec{k})$ is obtained from (45) and (46) by the replacements

$$\hat{x}(z_{sub}, p, k) \rightarrow \widehat{X}(z_{sub}, p, k) := \hat{x}(z_{sub}, p, k) - \hat{x}(z_{sub}^{os} := e_N(p), p, k) \quad (56)$$

for $x \in \{\alpha, \beta, \gamma, \delta, \epsilon\}$ and $X \in \{A, B, C, D, E\}$, where the isospin structure of $\widehat{A}, \dots, \widehat{E}$ is parametrized in analogy to (47) introducing isoscalar and isovector parts A^s, \dots, E^s and A^v, \dots, E^v , respectively.

We would like to remind the reader that offshell effects arise from two sources in our model. The first one comes from the purely hadronic renormalization factors \widehat{R} in the initial and final states and the second one from the loop contribution to the electromagnetic current. In the usual treatment without offshell effects like in [16], one neglects in (55) the term $\mathcal{J}_{loop, sub}^\mu$ and substitutes \widehat{R} by one.

As last topic in this section we will study the question of gauge invariance. By a straightforward calculation, one obtains for the loop contributions ($\rho \equiv J^0$)

$$\begin{aligned} \vec{k} \cdot \sum_{j=2}^9 \widehat{J}_j^{N[1]}(z, \vec{k}) &= \sum_{i=1,2} V_{eff}^{\pi dis}(i, z) \rho_{real}(i, \vec{k}) - \sum_{i=1,2} \rho_{real}(i, \vec{k}) V_{eff}^{\pi dis}(i, z - k) \\ &+ k \sum_{j=2}^9 \rho_j^{N[1]}(z, \vec{k}) + \mathcal{B}(z_f, \vec{k}) + \widehat{\mathcal{O}}\left(\frac{1}{M_N^3}\right), \end{aligned} \quad (57)$$

with the retarded disconnected π -loop contribution

$$V_{eff}^{\pi dis}(i, z) = v_{\bar{N}X_\pi}^0(i) G_0(z) v_{X_\pi \bar{N}}^0(i) \quad (58)$$

and the auxiliary quantity

$$\begin{aligned} \mathcal{B}(z, \vec{k}) &= \sum_{i=1,2} \left\{ \left(v_{\bar{N}X_\pi}^{0 nonrel}(i) G_0(z) v_{X_\pi X_{\pi\pi}}^0(i) G_0(z) \rho_{X_{\pi\pi} \bar{N}}^{(0)}(\vec{k}) \right) (z - k - H_{0 \bar{N} \bar{N}}) \right. \\ &\left. - (z - H_{0 \bar{N} \bar{N}}) \left(\rho_{\bar{N}X_{\pi\pi}}^{(0)}(\vec{k}) G_0(z - k) v_{X_{\pi\pi} X_\pi}^{0 nonrel}(i) G_0(z - k) v_{X_\pi \bar{N}}^0(i) \right) \right\}. \end{aligned} \quad (59)$$

In analogy to the corresponding discussion for the retarded MEC in [16], we would like to mention that the matrix element of $\mathcal{B}(z, \vec{k})$ vanishes between plane waves only, which fact indicates that additional loop contributions of at least fourth order in the pion-nucleon coupling are needed in order to fulfill gauge invariance. As has been indicated in (57), there exist additional sources for the breaking of gauge invariance in the order $1/M_N^3$. They have their origin in the fact that in the loop corrections the nonrelativistic expressions for the pion-nucleon vertex and for the momentum-energy relation of the intermediate nucleon are used whereas in $V_{eff}^{\pi dis}(z)$, which enters into our hadronic interaction (Elster potential, see [15] for further details), the relativistic expressions have been kept.

In our explicit evaluations, we have used the Siegert decomposition of the electric multipoles with the help of the relation

$$\langle \alpha_W | \vec{k} \cdot \left[\vec{J}_{eff}^{N[1]}(z, \vec{k}) + \vec{J}_{eff}^{N[2]}(z, \vec{k}) \right] | \alpha_{W-k} \rangle = \langle \alpha_W | k \left[\mathcal{J}_{eff}^{N[1]0}(z, \vec{k}) + \mathcal{J}_{eff}^{N[2]0}(z, \vec{k}) \right] | \alpha_{W-k} \rangle, \quad (60)$$

where $z = W + i\epsilon$. Here, $\mathcal{J}_{eff}^{N[1]\mu}(z, \vec{k})$ is given by (55) and $\mathcal{J}_{eff}^{N[2]0}(z, \vec{k})$ and $\vec{J}_{eff}^{N[2]}(z, \vec{k})$ denote the retarded two-body charge and currents given in equation (40) of [16], multiplied in addition by $\widehat{R}(z)$ from the left and by $\widehat{R}(z - k)$ from the right according to (30). If the Δ -isobar as well as the interaction V_{XX}^0 are ignored and if only pions are considered as explicit mesonic degrees of freedom, (60) can be derived rigorously in the leading order $1/M_N$ exploiting (57) and the similar expression for the retarded MEC of [16]. However, we use the Siegert decomposition (60) also in our full model. Thereby, as it is well-known, at least a part of the neglected currents like heavy-meson exchange contributions can be taken into account implicitly. We would like to emphasize that (57) is violated even in the leading order $1/M_N$ if the counter current $J_{counter}^\mu$ is set equal to zero.

Finally, we would like to remark that of the currents of leading relativistic order, the important spin-orbit current [19,20] is of course included in our numerical evaluation.

V. RESULTS FOR THE LOOP CONTRIBUTIONS

For the explicit calculation, we have chosen a reference frame where the two baryons have total momentum zero after the absorption of the photon. To begin the discussion we present in Figs. 7 through 11 our results for the quantities $\hat{A}(z_{sub}, p', k), \dots, \hat{E}(z_{sub}, p', k)$ of (56), which enter into the effective current in (55) via the contribution $\mathcal{J}_{loop, sub}^{N\mu}(z, \vec{k})$. In this context, one should remember that p' is the absolute value of the struck nucleon momentum after the absorption of the photon. Due to the chosen reference frame, $-\vec{p}'$ is the momentum of the spectator nucleon, so that z_{sub} is not an independent variable but determined by p' and k :

$$z_{sub} \equiv z_{sub}(k, p') = W - \sqrt{M_N^2 + p'^2} + i\epsilon, \quad (61)$$

with the invariant energy

$$W = \sqrt{M_d^2 + 2M_d k_{lab}}, \quad (62)$$

where M_d and k_{lab} denote the deuteron mass and the lab photon energy, respectively. The latter is related to k , the c. m. photon energy, via

$$k = k_{lab} \frac{M_d}{W}. \quad (63)$$

Therefore, the functions $\hat{A}(z_{sub}, p, k), \dots, \hat{E}(z_{sub}, p, k)$ can be treated effectively as functions solely of k and p' . For later purposes, we introduce in addition the so-called pole momentum p_0 via

$$W = 2\sqrt{M_N^2 + p_0^2}. \quad (64)$$

It is identical to the asymptotic relative momentum of the outgoing nucleons in photodisintegration. Due to (56), the functions \hat{A}, \dots, \hat{E} are equal to zero at p_0 . Moreover, they vanish for k and $p' \rightarrow 0$. Therefore, as we will see in the next section, the loop contributions do not play any role in the observables at low energies small compared to the π -threshold. For increasing energy, the analytical behavior of \hat{A}, \dots, \hat{E} as a function of k shows in general a more and more pronounced slope. Beyond π -threshold, there exists for momenta $p' < p_{max}(k)$ for certain values of p_{max} smaller than p_0 an imaginary part due to occurring singularities in the pion-loops. In the Δ -region, its absolute size is in general of the same order of magnitude than the corresponding real parts. Moreover, for small p' the absolute size of the functions depicted in Figs. 7 through 11 is comparable to the corresponding values (3) of the charge and the anomalous magnetic moment of the nucleon.

Besides the electromagnetic loop contributions $\mathcal{J}_{loop, sub}(z, \vec{k})$ entering (55), an additional new feature of our effective one-body current, compared to the conventional onshell expression, is the occurrence of the dressing operator \hat{R} , appearing before (*i*) and after (*f*) photon absorption and described according to (24) by $R_i(z, \vec{p}_1, \vec{p}_2)$ and $R_f(z, \vec{p}'_1, \vec{p}'_2)$, respectively. Whereas $R_f = R_f(k, p')$ depends only on k and p' , because $p'_1 = p'_2 \equiv p'$ and $z = \sqrt{M_d^2 + k^2} + k + i\epsilon$, one finds that $R_i = R_i(k, p', x)$ depends also via $x = \hat{p}' \cdot \hat{k}$ on the angle between \hat{p}' and \hat{k} , because the deuteron is not in its rest frame. In general, as becomes evident in Fig. 12, one notes that $R_f(k, p')$ is smaller or larger than 1 for momenta p' smaller or larger than the onshell value p_0 , respectively, whereas $R_i(k, p', x)$ in the initial state is always larger than 1, leading therefore to a considerable amplification of the loop contribution $\mathcal{J}_{loop, sub}(z, \vec{k})$ in (55). In this context we would like to point out another interesting feature of the dressing factors, namely if the outgoing nucleons are onshell, i.e. $R_f(k, p_0) = 1$, the value of the corresponding dressing factor $R_i(k, p_0, x)$ is not equal to one, indicating that one of the initial nucleons has to be offshell. This behavior can well be understood by remembering that the absorption of a *real* photon by a free nucleon is not possible without internal excitation.

Finally, we would like to discuss the matrixelement of the quantity $\hat{R}(z - k)/\hat{R}(z^{os} - k)$, i.e.

$$\langle \bar{N}(-\vec{p}') | \bar{N}(\vec{p}' - \vec{k}) | \frac{\hat{R}(z - k)}{\hat{R}(z^{os} - k)} | \bar{N}(-\vec{p}) | \bar{N}(\vec{p} - \vec{k}) \rangle = \delta(\vec{p}' - \vec{p}) K(z - k, p', k, \hat{p}' \cdot \hat{k}), \quad (65)$$

which appears in (55). According to Fig. 13, K is smaller than 1 in the most relevant momentum range $p' < p_0$, leading therefore to a weakening of the contribution of $j_{real}^{nr, \mu}$ in (55). In contrast to R_i , the function K is almost independent of $x = \hat{p}' \cdot \hat{k}$.

VI. OFFSHELL EFFECTS IN DEUTERON PHOTODISINTEGRATION

To begin with, we will describe very briefly the ingredients of the adopted hadronic interaction model for which we use the model “CC(ret2)” of [16] as our reference point for offshell effects. It incorporates full retardation in potentials and two-body currents, π - as well as ρ -exchange in the $N\Delta$ -interaction and the coupling to the πd -channel. For the effective nucleon one-body current, the usual onshell expression including spin-, convection- and the spin-orbit currents. Any offshell effects from the electromagnetic pion-loops or from the dressing operator are neglected.

We now turn to the discussion of our numerical results. We indicate by a superscript “onsh” or “offsh” in the captions of Figs. 14 through 17 whether the considered observable is calculated using the conventional onshell current or in the offshell approach (55) for the effective one-body current, respectively. First, we will consider the total cross section for photodisintegration presented in Fig. 14. In order to show more clearly the relative offshell effect, we show in Fig. 15 the ratio $\sigma_{\text{tot}}^{\text{offsh}}/\sigma_{\text{tot}}^{\text{onsh}}$. One readily notes that at low energies up to about $k_{\text{lab}} = 100$ MeV offshell effects are almost negligible. Even in the Δ region, up to about $k_{\text{lab}} = 300$ MeV, they do not exceed one percent, because the one-body nucleon current is of minor importance and offshell effects in the $\bar{N}\Delta$ -excitation are already included in the reference calculation [16]. Thus only beyond the Δ -peak offshell effects become more and more pronounced, leading to a sizeable reduction of about 10 percent at $k_{\text{lab}} = 500$ MeV. In the differential cross sections in Fig. 16 the offshell effects are most prominent at forward angles decreasing it up to about 30 % for the highest energy shown, whereas around 90° and at backward angles the effects are much smaller. Our detailed analysis shows that this result is the combined effect of various interferences. It turns out that the strong decrease at 0° for higher energies is mainly due to a constructive interference of the contributions proportional to \hat{A} (offshell correction to the charge) and \hat{D} (proportional to $\vec{\sigma} \times \vec{p}'$) whereas the other offshell corrections are of minor importance. On the other hand, at 90° the multiplication of $j_{\text{real}}^{N[1]\mu}$ by the factor $\hat{R}(z-k)/\hat{R}(z^{os}-k)$ in (55) leads to a considerable decrease of the cross section, which is, however, partially canceled by the offshell correction \hat{A} to the charge. In contrast to the differential cross section, the most interesting single particle polarization observables like the photon asymmetry Σ , the tensor target asymmetry T_{20} and the outgoing nucleon polarizations $P_y(n)$ and $P_y(p)$ are only moderately affected by offshell effects as is demonstrated in Fig. 17. Therefore, the incorporation of offshell effects in our framework does not resolve the discrepancy between theory and experiment in the proton polarization around 90° .

From these results, we may conclude that for an only qualitative understanding of deuteron photodisintegration, one may neglect offshell effects safely. However, for a precise theoretical interpretation of experimental data with an accuracy on the level of a few percent it is certainly necessary to take into account offshell effects as discussed in this work.

VII. SUMMARY AND OUTLOOK

In the present paper, we have investigated the importance of offshell effects in deuteron photodisintegration by evaluating one-pion loop contributions within a hadronic interaction model using mesons, nucleons, and Δ -isobars as effective degrees of freedom as developed in [15,16]. It is based on a conventional nonrelativistic time-ordered perturbation theory and allows a realistic description of hadronic and electromagnetic reactions on the two-nucleon system for energies up to about 500 MeV excitation energy.

The offshell effects discussed here consist of two parts, which both are related to the same basic meson-nucleon interaction mechanism:

(i) A purely hadronic offshell contribution arising from the presence of a “nucleon-meson cloud” as described by the “dressing factor” \hat{R} . It has its origin in the fact that the active nucleon, on which the photon is absorbed or emitted, is subject to initial and final state interactions in the presence of other baryons.

(ii) An electromagnetic offshell contribution arising from the absorption or emission of a photon by this meson cloud as described by the loop contributions to the e.m. current. By the inclusion of a suitably chosen counter current it is ensured that this loop contribution vanishes onshell so that the correct onshell properties of the physical nucleon are automatically preserved.

We would like to emphasize once more again, that such offshell effects depend on the hadronic interaction model and, therefore, as such are not separately observable. However, as our simple one-loop model

for the offshell effects has shown, they will influence theoretical predictions. Despite the simplicity of the present model, we expect that it is sufficiently realistic enough in order to allow a semiquantitative answer to the interesting question as to the size of offshell effects in electromagnetic reactions on bound systems.

Our results clearly show that for a theoretical understanding of this reaction within a, say, 20-30 percent accuracy, offshell effects can safely be neglected. They do not change qualitatively any of the observables, which we have studied, within that margin. On the other hand, these effects are not that small compared to the precision of present state-of-the-art experiments with an accuracy of better than 5 percent. In view of the fact, that we found within our framework offshell effects in observables of a size which lie in this range, we take this as a clear indication that for a theoretical interpretation of high precision data of the order of a few percent accuracy, offshell effects have to be taken into account consistently. But it is also clear, that in this case one needs a more realistic model for the internal structure of nucleons including a consistent treatment of offshell effects. It remains for future work to apply the present model to other e.m. reactions on the deuteron like electrodisintegration, pionproduction and Compton scattering.

- [1] A. M. Bincer, Phys. Rev. **118**, 855 (1960)
- [2] E. M. Nyman, Nucl. Phys. A **154**, 97 (1970)
- [3] E. M. Nyman, Nucl. Phys. A **160**, 517 (1971)
- [4] M. G. Hare, Ann. Phys. **74**, 595 (1972)
- [5] J. W. Bos and J. H. Koch, Nucl. Phys. A **563**, 539 (1993)
- [6] H. W. Naus and J. H. Koch, Phys. Rev. C **36**, 2459 (1987)
- [7] P. C. Tiemeijer and J. A. Tjon, Phys. Rev. C **42**, 599 (1990)
- [8] J. W. Bos, S. Scherer and J. H. Koch, Nucl. Phys. A **547**, 488 (1992)
- [9] H. C. Dönges, M. Schäfer and U. Mosel, Phys. Rev. C **51**, 950 (1995)
- [10] S. Kondratyuk, G. Martinus and O. Scholten, Phys. Lett. B **418**, 20 (1998)
- [11] H. W. Fearing, Few. Body Syst. Suppl. **12** (2000) 263
- [12] S. Scherer and H. W. Fearing, Nucl. Phys. A **684** (2001) 499
- [13] X. Song, J. P. Cheng and J. S. McCarthy, Z. Phys. A **341**, 275 (1992)
- [14] S. Kondratyuk, and O. Scholten, nucl-th/9906044v2
- [15] M. Schwamb and H. Arenhövel, nucl-th/9912017, accepted for publication in Nucl. Phys. A
- [16] M. Schwamb and H. Arenhövel, nucl-th/0008034, accepted for publication in Nucl. Phys. A
- [17] D. Schütte and J. da Providencia, Nucl. Phys. A **338**, 463 (1980)
- [18] C. Elster, W. Ferchländer, K. Holinde, D. Schütte, and R. Machleidt, Phys. Rev. C **37**, 1647 (1988)
- [19] A. Cambi, B. Mosconi, and P. Ricci, Phys. Rev. Lett. **48**, 462 (1982).
- [20] P. Wilhelm, W. Leidemann, and H. Arenhövel, Few-Body Syst. **3**, 111 (1988).
- [21] R. Crawford *et al.*, Nucl. Phys. A **603**, 303 (1996)
- [22] J. Arends *et al.*, Nucl. Phys. A **412**, 509 (1984)
- [23] G. Blanpied *et al.*, Phys. Rev. C **52**, R455 (1995); Phys. Rev. C **51**, 024604 (2000)
- [24] F. Adamian *et al.*, J. Phys. G **17**, 1189 (1991)
- [25] H. Ikeda *et al.*, Phys. Rev. Lett. **42**, 1321 (1979)
- [26] A. S. Bratashvskii *et al.*, Sov. J. Nucl. Phys. **32**, 216 (1980)

APPENDIX A: SOME TECHNICAL DETAILS

In this appendix, we illustrate the explicit evaluation of the functions $\hat{\alpha}, \dots, \hat{\epsilon}$ in (45) and (46). As an example, we study the contribution $J_6^{N[1]\mu}(z, \vec{k})$ (see (38) and Fig. 6). First, we split $J_6^{N[1]\mu}(z, \vec{k})$ into one-body contributions, i.e.

$$J_6^{N[1]\mu}(z, \vec{k}) = \sum_{i=1,2} j_6^{N[1]\mu}(z, \vec{k}, i) \quad (66)$$

where, the argument i denotes the “active” nucleon absorbing the photon. The relevant hadronic and electromagnetic interactions are given by the renormalized nonrelativistic πN -vertex

$$\langle \bar{N}(\vec{p}') | v_{\bar{N}Q_\pi}^{nonrel} | \pi(\vec{q}, \mu) \bar{N}(\vec{p}) \rangle = \delta(\vec{p}' - \vec{p} - \vec{q}) \frac{g_\pi}{2M_N} \tau_\mu i \vec{\sigma} \cdot \vec{q} F_\pi(\vec{q}^2) \quad (67)$$

and the Kroll-Rudermann current contribution

$$\langle \pi(\vec{q}, \mu) \bar{N}(\vec{p}') | \rho_{Q_\pi \bar{N}}^{(1)}(\vec{k}) | \bar{N}(\vec{p}) \rangle = 0, \quad (68)$$

$$\langle \pi(\vec{q}, \mu) \bar{N}(\vec{p}') | \vec{j}_{Q_\pi \bar{N}}^{(1)}(\vec{k}) | \bar{N}(\vec{p}) \rangle = \delta(\vec{q} - \vec{p} + \vec{k} + \vec{p}') \frac{g_\pi}{2M_N} (-)^\mu [\hat{e}, \tau_{-\mu}] i \vec{\sigma} F_\pi(\vec{q}^2), \quad (69)$$

where μ denotes the charge of the pion and τ_μ are the usual Pauli-matrices in the spherical basis. The hadronic form factor

$$F_\pi(\vec{q}^2) = \left(\frac{\Lambda_\pi^2 - m_\pi^2}{\Lambda_\pi^2 + \vec{q}^2} \right)^2, \quad \Lambda_\pi = 1700 \text{ MeV}, \quad (70)$$

is taken consistently from the Elster potential (Table I in [15]). Then, we obtain in the c.m. frame of the final state the following expression for $j_6^{N[1]\mu}(z, \vec{k})$:

$$\langle \bar{N}(\vec{p}') | j_6^{N[1]0}(z, \vec{k}) | \bar{N}(\vec{p}) \rangle = 0, \quad (71)$$

$$\langle \bar{N}(\vec{p}') | \vec{j}_6^{N[1]}(z, \vec{k}) | \bar{N}(\vec{p}) \rangle = \delta(\vec{p} + \vec{k} - \vec{p}') \frac{e\tau_0 g_\pi^2}{2M_N^2} \int d^3 q \vec{\Upsilon}(\vec{p}', \vec{q}) \quad (72)$$

with $(\omega_\pi(x) = \sqrt{m_\pi^2 + x^2})$

$$\vec{\Upsilon}(\vec{p}', \vec{q}) := \frac{F_\pi^2(\vec{q}^2)}{(2\pi)^3 2\omega_\pi(\vec{q})} \frac{\vec{\sigma} \cdot \vec{q} \vec{\sigma}}{z_{sub} - M_N - \frac{(\vec{p}' - \vec{q})^2}{2M_N} - \omega_\pi(\vec{q})}, \quad (73)$$

where for the sake of simplicity the argument i in $j_6^{N[1]\mu}(z, \vec{k}, i)$ denoting the ‘‘active’’ nucleon (see (66)) has been skipped.

Note that we use the nonrelativistic energy-momentum relation for the ‘‘active’’ nucleon; z_{sub} is given by (61). Concerning the dependence of $\vec{\Upsilon}(\vec{p}', \vec{q})$ on the angle $x := \hat{p}' \cdot \hat{q}$, we make use of the Legendre polynomial expansion

$$\vec{\Upsilon}(\vec{p}', \vec{q}) \equiv \vec{\Upsilon}(p', q, x) = \sum_{\Lambda=0}^{\infty} \vec{\Upsilon}_\Lambda(p', q) P_\Lambda(x) \quad (74)$$

with

$$\vec{\Upsilon}_\Lambda(p', q) = \frac{2\Lambda + 1}{2} \int_{-1}^1 dy \vec{\Upsilon}(p', q, y) P_\Lambda(y). \quad (75)$$

With the help of

$$\int d\Omega_q \vec{\sigma} \cdot \hat{q} P_\Lambda(\hat{p}' \cdot \hat{q}) = \frac{4\pi}{3} \vec{\sigma} \cdot \hat{p}' \delta_{\Lambda 1} \quad (76)$$

one obtains after some straightforward algebra

$$\begin{aligned} \langle \bar{N}(\vec{p}') | \vec{j}_6^{N[1]}(z, \vec{k}) | \bar{N}(\vec{p}) \rangle &= \delta(\vec{p} + \vec{k} - \vec{p}') \frac{e\tau_0 g_\pi^2}{16\pi^2 M_N^2} \vec{\sigma} \cdot \hat{p}' \vec{\sigma} \\ &\times \int dq \frac{q^3 F_\pi^2(\vec{q}^2)}{\omega_\pi(q)} \int_{-1}^1 dy \frac{y}{z_{sub} - M_N - \frac{p'^2}{2M_N} - \frac{q^2}{2M_N} + \frac{p'qy}{M_N}}. \end{aligned} \quad (77)$$

The integral over y can be evaluated with the help of the general formula

$$\int_{-1}^1 dx \frac{\phi(x)}{x - x_0 + i\epsilon} = \mathbf{P} \int_{-1}^1 dx \frac{\phi(x)}{x - x_0} + \phi(x_0) \ln \left| \frac{1 - x_0}{1 + x_0} \right| - i\pi \phi(x_0). \quad (78)$$

Therefore, one obtains both real and imaginary parts for the current contribution. Finally, with the help of

$$\vec{\sigma} \cdot \hat{p}' \vec{\sigma} = \hat{p}' + i \vec{\sigma} \times \hat{p}' , \quad (79)$$

one obtains the contributions of $\vec{j}_6^{N[1]}(z, \vec{k})$ to the functions $\hat{\alpha}, \dots, \hat{\epsilon}$. Concerning the other loop contributions in Fig. 6, we would like to note that in general not only one, but two or even three angles between the momenta, i.e. $\hat{k} \cdot \hat{p}'$, $\hat{q} \cdot \hat{p}'$, $\hat{k} \cdot \hat{q}$ occur in the corresponding propagators, yielding therefore much more complicated expressions. Nevertheless, the general principle of evaluating these loop contributions is the same as for $\vec{j}_6^{N[1]}(z, \vec{k})$.

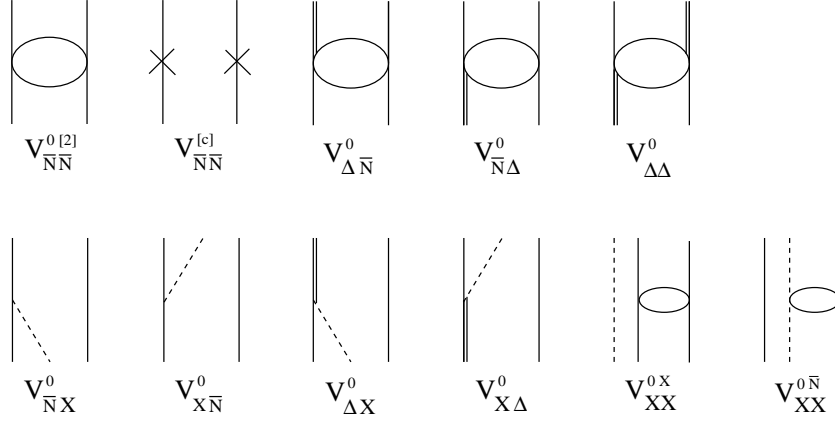


FIG. 1. Diagrammatic representation of the various components of V^0 . The open ellipse symbolizes a given hermitean two-body interaction. The one-nucleon counter term $v^{[c]}$ is indicated by a cross.

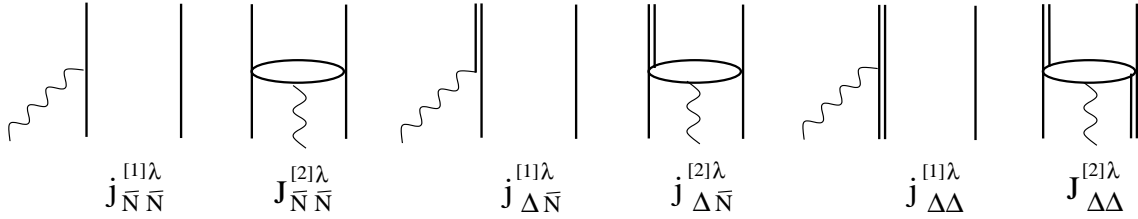


FIG. 2. Diagrammatic representation of the baryonic currents. An open ellipse symbolizes a two-body exchange current, generated for example by heavy meson exchange.

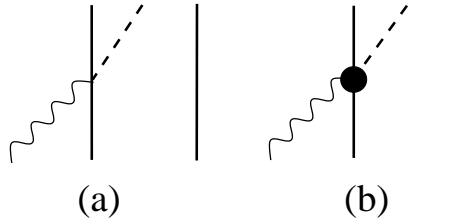


FIG. 3. Diagrammatic representation of the meson production currents $J_{X\bar{N}}^\mu$: (a) contact current $j_{X\bar{N}}^{(1)\mu}$ and (b) vertex current $j_{X\bar{N}}^{(1v)\mu}$.

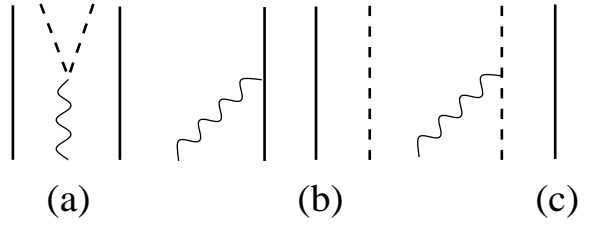


FIG. 4. Diagrammatic representation of (a) the two-meson production current $j_{X\bar{X}}^{(0)\mu}$, and the current components $J_{X\bar{X}}^\mu$: (b) nucleon current $j_{X\bar{X}}^{\bar{N}\mu}(\vec{k})$, (c) meson current $j_{X\bar{X}}^{X\mu}(\vec{k})$.

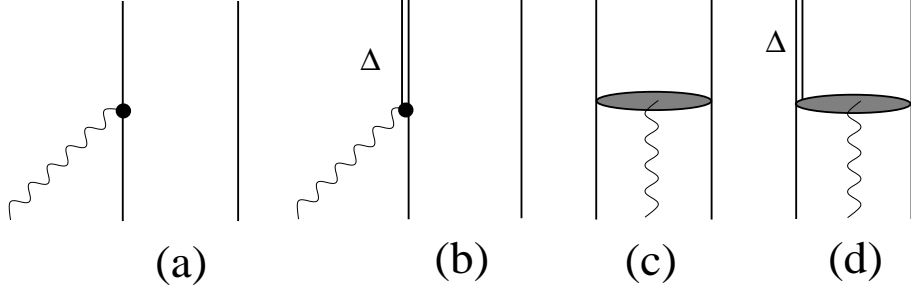


FIG. 5. Diagrammatic representation of the separate contributions to the effective current operator $J_{eff}^\mu(z, \vec{k})$ (see Eq. (31)): (a) $J_{eff}^{N[1]\mu}(z, \vec{k})$, (b) $J_{eff}^{\Delta[1]\mu}(z, \vec{k})$, (c) $J_{eff}^{N[2]\mu}(z, \vec{k})$, and (d) $J_{eff}^{\Delta[2]\mu}(z, \vec{k})$.

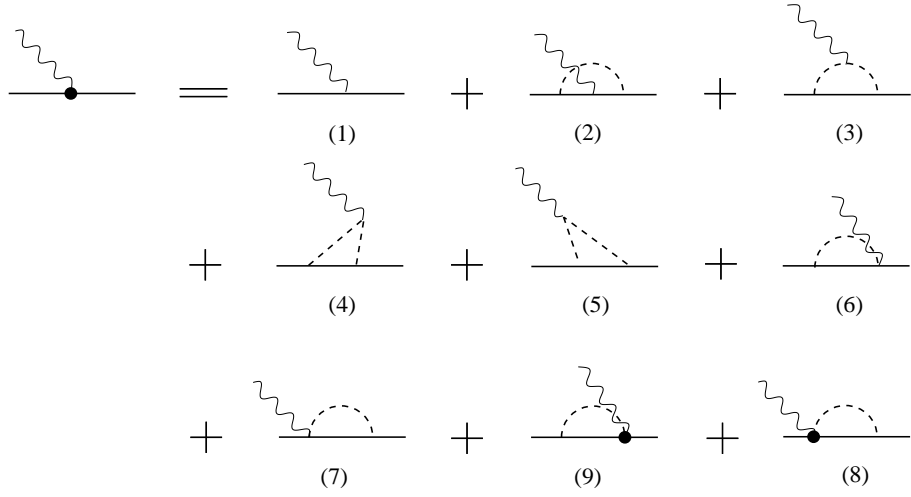


FIG. 6. Diagrammatic representation of the separate contributions to the effective nucleonic one-body current $J_{eff}^{N[1]\mu}(z, \vec{k})$ (equations (33) through (41)), represented in contrast to the bare nucleon current by a filled circle.

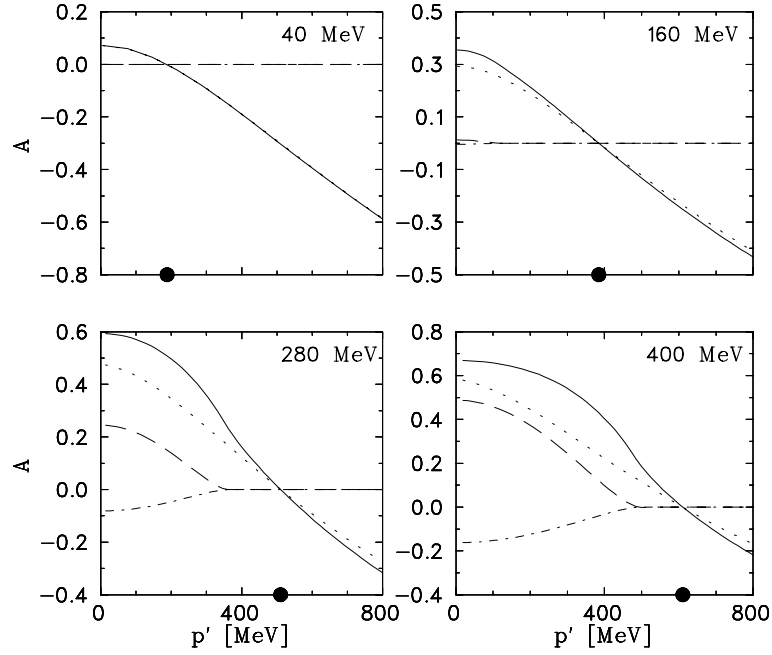


FIG. 7. The isospin components of the function $\hat{A}(p', k)$ (56) of the effective loop current $\mathcal{J}_{loop, sub}^{N\mu}(z, \vec{k})$ for various laboratory energies k_{lab} of the incoming photon. Notation of the curves: solid: real part A^s , dashed: imaginary part A^s , dotted: real part A^v , dash-dotted: imaginary part A^v . The location of the onshell momentum p_0 of the outgoing nucleon, defined in (64), is indicated by a filled circle.

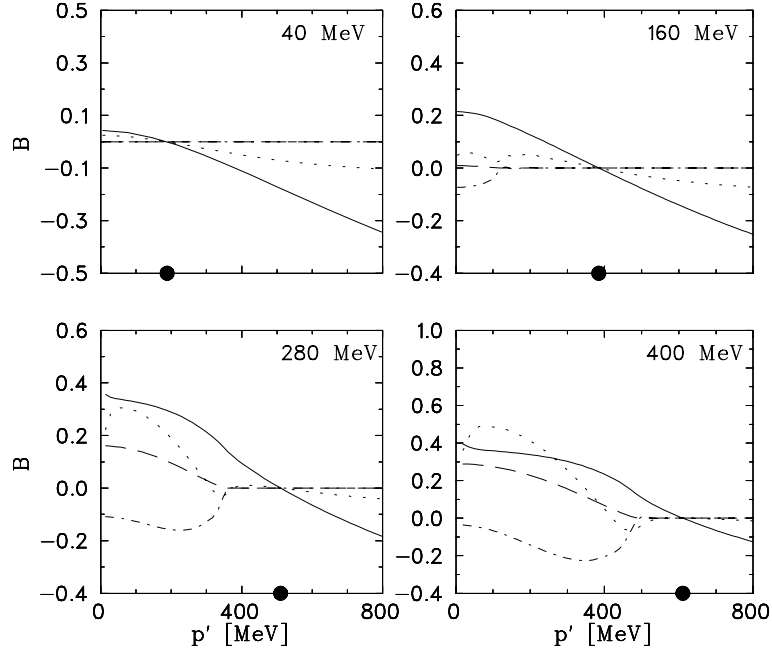


FIG. 8. The isospin components of the function $\hat{B}(p', k)$ (56) of the effective loop current for various laboratory energies k_{lab} of the incoming photon. Notation of the curves in analogy to Fig. 7.

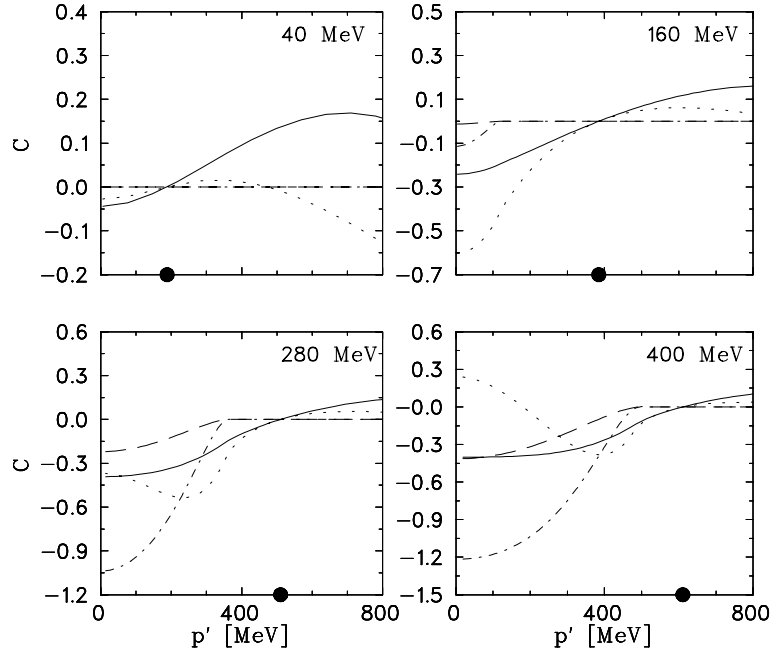


FIG. 9. The isospin components of the function $\hat{C}(p', k)$ (56) of the effective loop current for various laboratory energies k_{lab} of the incoming photon. Notation of the curves in analogy to Fig. 7.

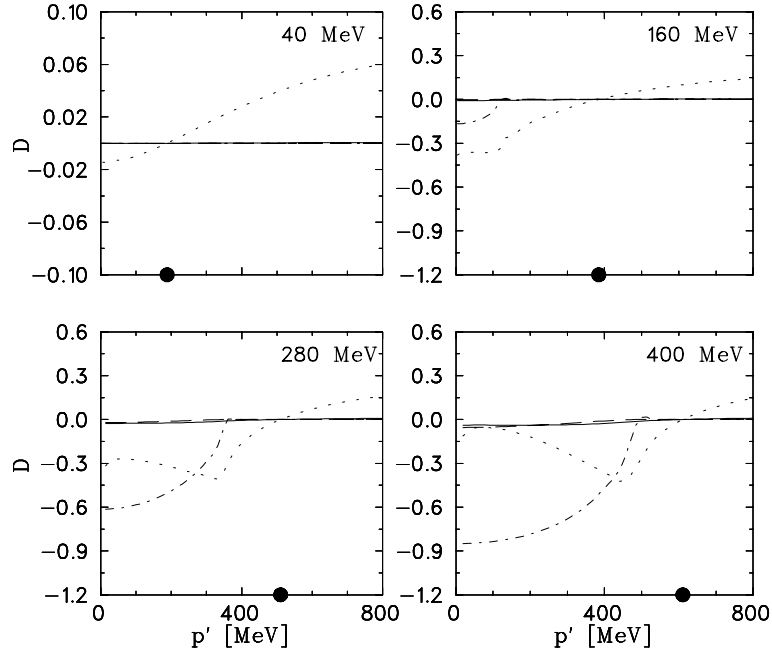


FIG. 10. The isospin components of the function $\hat{D}(p', k)$ (56) of the effective loop current for various laboratory energies k_{lab} of the incoming photon. Notation of the curves in analogy to Fig. 7.

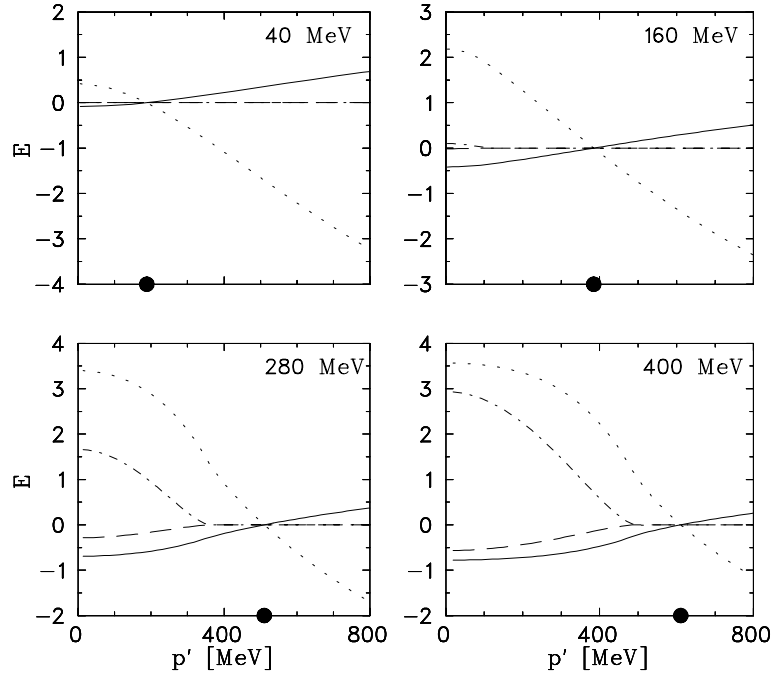


FIG. 11. The isospin components of the function $\hat{E}(p', k)$ (56) of the effective loop current for various laboratory energies k_{lab} of the incoming photon. Notation of the curves in analogy to Fig. 7.

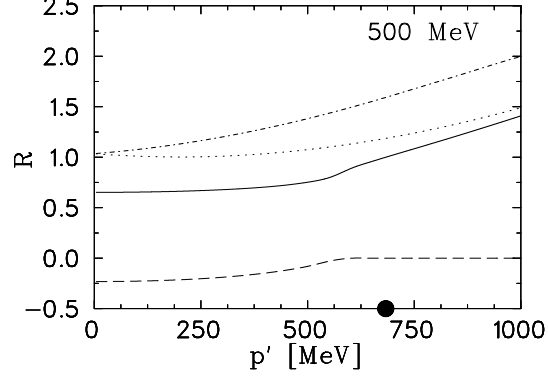


FIG. 12. The matrix element (25) of the dressing factor for $k_{lab} = 500$ MeV. Notation of the curves: solid: real part of $R_f(k, p')$, dashed: imaginary part of $R_f(k, p')$, dotted: $R_i(z - k, p', k, x = 1)$, dash-dotted: $R_i(k, p', x = -1)$. R_i has no imaginary part. The location of the onshell momentum p_0 of the outgoing nucleon is indicated by a filled circle.

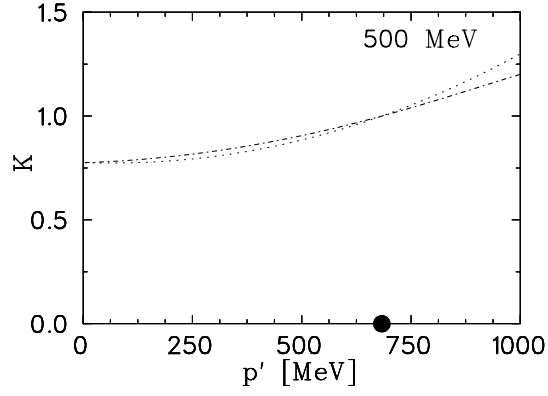


FIG. 13. The function K (65) for $k_{lab} = 500$ MeV. Notation of the curves: dotted: $K(z - k, p', k, x = 1)$, dash-dotted: $K(z - k, p', k, x = -1)$. K has no imaginary part. The location of the onshell momentum p_0 of the outgoing nucleon is indicated by a filled circle.

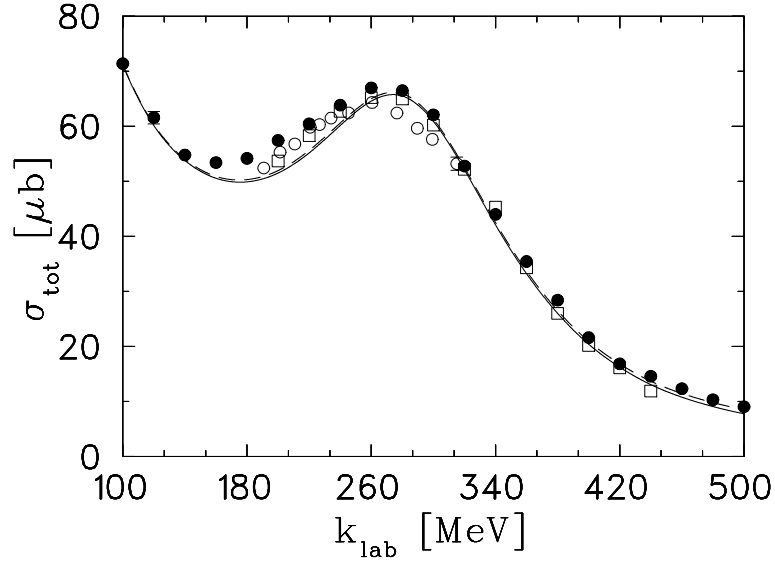


FIG. 14. Total cross section $\sigma_{tot}(\gamma d \rightarrow NN)$ of deuteron photodisintegration. Notation of the curves: dashed: σ_{tot}^{onsh} , solid: σ_{tot}^{offsh} . Experimental data from [21] (●), [22] (□) and [23] (○).

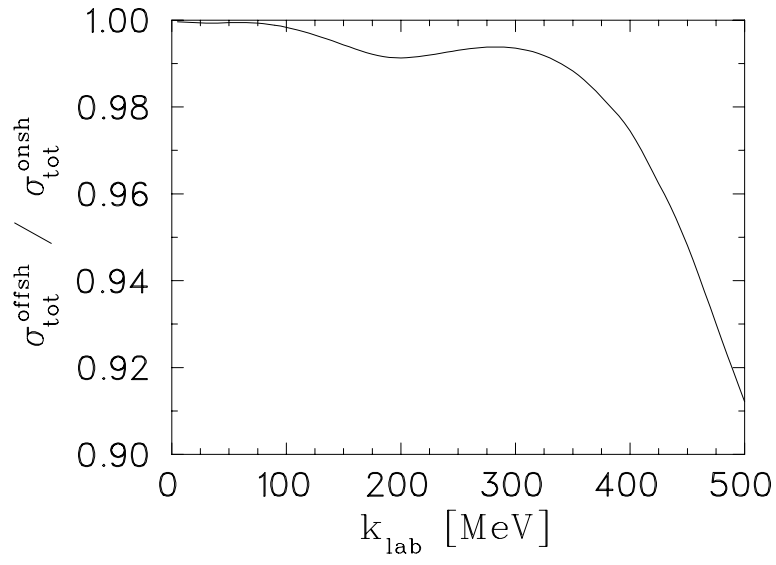


FIG. 15. Ratio $\sigma_{\text{tot}}^{\text{offsh}} / \sigma_{\text{tot}}^{\text{onsh}}$ of the total cross section of deuteron photodisintegration.

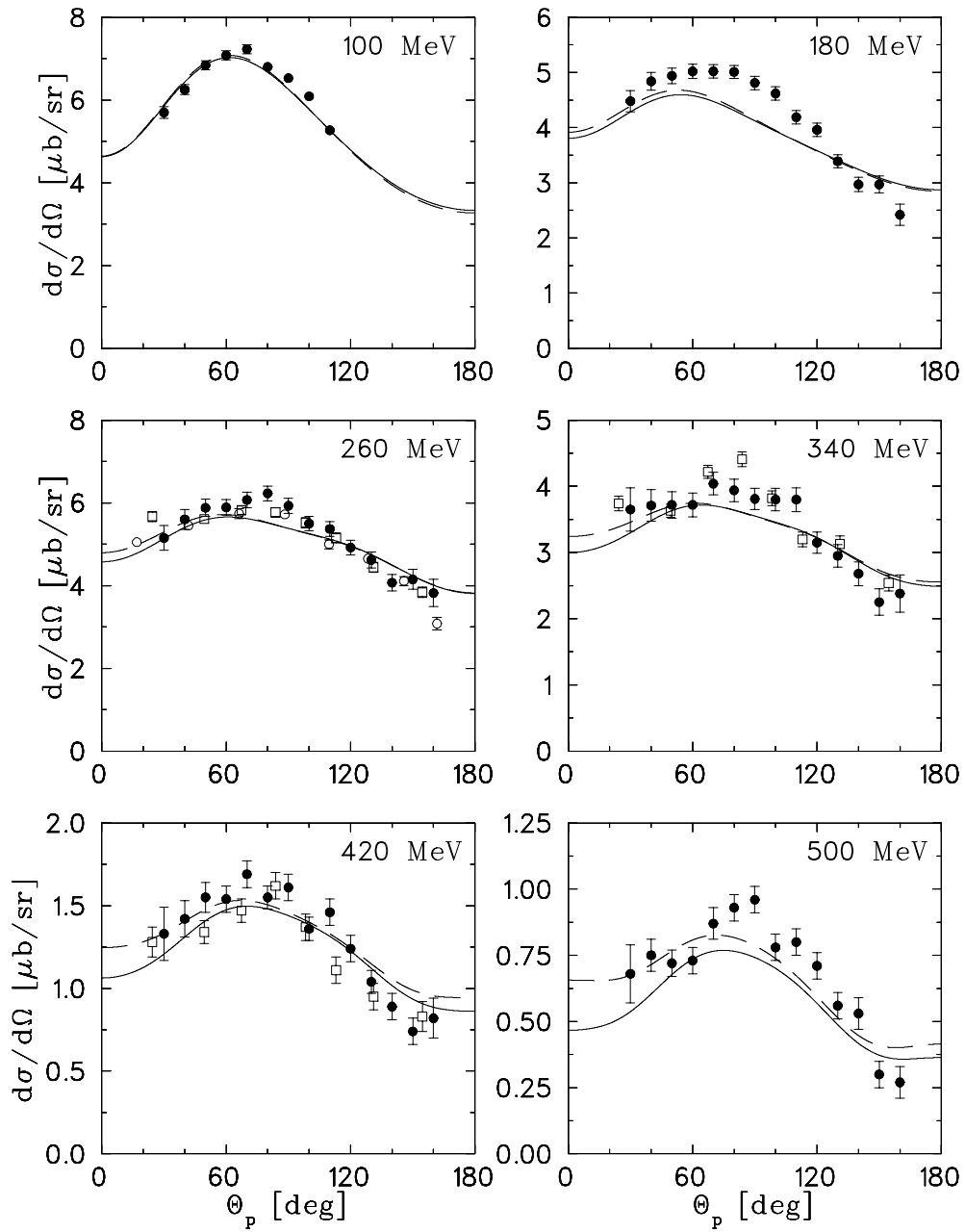


FIG. 16. Differential cross sections of deuteron photodisintegration for various energies. Notation of the curves and experimental data as in Fig. 14.

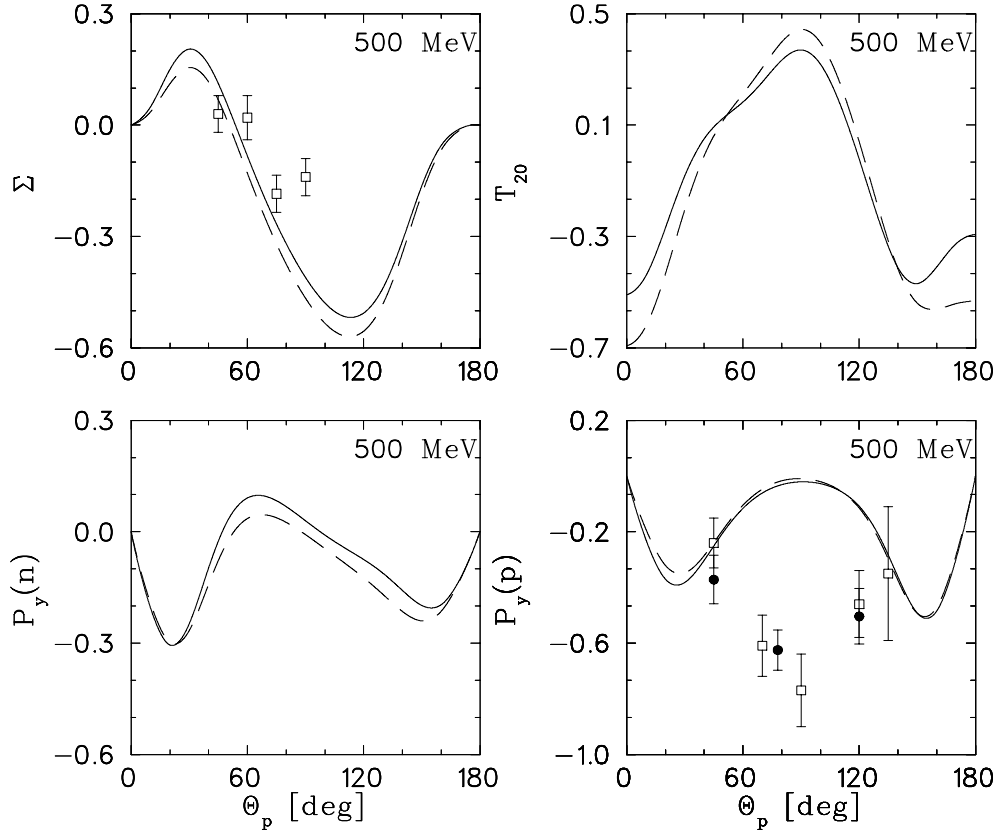


FIG. 17. Linear photon asymmetry Σ , tensor target asymmetry T_{20} , neutron polarization $P_y(n)$ and proton polarization $P_y(p)$ in deuteron photodisintegration for $k_{lab} = 500$ MeV. Notation of the curves as in Fig. 14. Experimental data for Σ from [24] (\square), for $P_y(p)$ from [25] (\square) and [26] (\bullet).